



# Choline chloride-coated UiO-66-Urea MOF: A novel multifunctional heterogeneous catalyst for efficient one-pot three-component synthesis of 2-amino-4*H*-chromenes

Mohadeseh Akbarian, Esmael Sanchooli <sup>\*</sup>, Ali Reza Oveisi <sup>\*</sup>, Saba Daliran

Department of Chemistry, University of Zabol, P.O. Box: 98615-538, Zabol, Iran

## ARTICLE INFO

### Article history:

Received 22 September 2020

Received in revised form 19 December 2020

Accepted 26 December 2020

Available online 30 December 2020

### Keywords:

Metal-organic frameworks

Zirconium-based MOF

Ionic liquid incorporation in MOF

Deep-eutectic solvent

Hybridization

Multi-component reactions (MCRs)

## ABSTRACT

A new Zr-based MOF, namely, UiO-66-Urea, was prepared through polymerization between the 2-aminoterephthalate linkers of UiO-66-NH<sub>2</sub> MOF and 1,4-phenylene diisocyanate under mild reaction conditions. Post-synthetic coating of UiO-66-Urea with choline chloride (ChCl), as easily available, inexpensive, and nontoxic reagent, under thermal and solvent-free conditions resulted in *in-situ* formation of a deep-eutectic solvent-like on the UiO-66-Urea's surface, called here ChCl@UiO-66-Urea. The presence of Zr<sub>6</sub>O<sub>4</sub>(OH)<sub>4</sub> nodes and urea groups may capable of strong hydrogen bond formation with ChCl. The porous and bioinspired ChCl@UiO-66-Urea was characterized using FT-IR, powder XRD, SEM, EDX elemental mapping, TGA, and BET surface area measurements. Choline chloride-coated UiO-66-Urea was successfully promoted one-pot three-component synthesis of 2-amino-4*H*-chromenes, as biologically active heterocycles, through reactions of aldehydes, malononitrile, and  $\alpha$ -naphthol or 4-hydroxycoumarin under solvent-free conditions. The catalytic activity of the respective solid was superior than UiO-66, UiO-66-NH<sub>2</sub>, UiO-66-Urea, and even ChCl-2Urea due to synergistic effect between actives sites of UiO-66-Urea and ChCl. The reaction includes a consecutive three-step Knoevenagel condensation/Michael addition/cyclization mechanism.

© 2020 Elsevier B.V. All rights reserved.

## 1. Introduction

Porous metal-organic frameworks (MOFs) are a class of micro/mesoporous materials formed in a highly ordered manner by coordination bond reactions between metal ions/nodes and organic linkers [1–3]. MOFs are able to be tailored through the choose control of organic linkers and metal ions for desired chemical process. As a result, within a short span of time, they have been gained much attention in a wide research area including catalysis [4–9], photocatalysis [10,11], separation [12], chemical sensing [13], drug delivery [14,15], toxic compounds remediation [16] and so on. Surface functionality and incorporation of a variety of functional moieties in MOFs are the other key advantages of them [17]. The organic struts and the clusters can be post-synthetically modified (PSM) with different species to make functionalized MOFs which offers advantages over the pristine MOFs [18]. Zr-based MOFs and at the top of them, UiO-66 (UiO = University of Oslo) series [19–21] have dramatically gained attention

span because of their high surface area, high thermal and chemical stability, and low toxicity.

Ionic liquids (ILs) are environment-friendly and new class of solvents with significant properties such as low volatility, high thermal and chemical stability, and high polarity which make them as appropriate solvents and/or catalysts for diverse chemical reactions [22]. Deep eutectic solvents (DESs) are a new emerging class of ionic liquids which obtained from a eutectic mixture of self-assembling two or more Brønsted/Lewis acids and bases through hydrogen bonding formation without the need of any solvent and the further purification [23]. They share many features and properties with ILs but, in contrast, they can include a wide range of anionic and/or cationic species. As a result, they have been considered by researchers in significant areas in concept of green and sustainable chemistry. However, ILs also have some limitations in industrial applications due to their high viscosity and their problematic recovery from the reaction mixture, and low efficiency/selectivity. To address these drawbacks, ILs can be confined into MOFs, namely "IL incorporation in MOFs" [24], collecting the advantages of both ILs and MOF structures within a new material, IL/MOF composite [25,26]. They have thus recently emerged as promising materials for potential applications including adsorption [27,28] and catalysis [8,24,29]. Nevertheless, in spite of these achievements, this strategy mainly is

<sup>\*</sup> Corresponding authors.

E-mail addresses: [Esmael\\_sanchooli@uoz.ac.ir](mailto:Esmael_sanchooli@uoz.ac.ir) (E. Sanchooli), [aroveisi@uoz.ac.ir](mailto:aroveisi@uoz.ac.ir) (A.R. Oveisi).

limited to the use of ILs and further the integrating the two individual components together by PSM procedures to give the desired material. Also, the simple inclusion of ILs into MOFs void space can be led to the lack of maximum accessibility to internal pores.

Chromenes are an important class of heterocyclic compounds with enormous variety of biologically activities such as antimicrobial, anti-cancer, antibacterial, anti-rheumatic and anti-allergic activities [30–37]. They also have been used in agrochemicals, pharmaceutical and synthetic drugs such as Alzheimer's disease and Huntington's disease [31,38–41]. Some of relevant biological and pharmacological active structures are presented in Fig. 1.

Thus, over the years, many catalysts such as  $\text{InCl}_3$  [42],  $\text{I}_2/\text{K}_2\text{CO}_3$  [43], nanostructured diphosphate  $\text{Na}_2\text{CaP}_2\text{O}_7$  (DIPH) [44], sodium-modified hydroxyapatite [45], KG-60-piperazine [46], alkylaminopyridine-grafted on HY Zeolite [47], heteropolyacid [48], triazine functionalized ordered mesoporous organosilica [49], and Laccase immobilized on  $\text{CoFe}_2\text{O}_4\text{-KCC-1}$  [50] have been reported for the synthesis of 2-amino-4*H*-chromenes. On other hand, porous materials such as tungstic acid functionalized mesoporous SBA-15 [51], zinc-based MOF [52], mordenite zeolite/MIL-101(Cr) composite [53], Er-based MOF [54], and triazine-based porous organic polymer (POP) [55] have been used to promote the synthesis of other chromene derivatives with different compositions. However, these methods suffer from some drawbacks such as the use of additive/toxic reaction media and/or toxic reagent, not easily available catalyst/reagent, low efficiency, long reaction times, high loading and/or non-reusability of used catalyst, and tedious procedure. In addition, MOFs with divalent Zn(II) ions are not stable under many conditions, which has become a major concern for the their applications in divers areas [56].

Taking into consideration of the above-mentioned, we present herein, for the first time, an effective design of porous and bioinspired  $\text{ChCl}@\text{UiO-66-Urea}$ , deep eutectic solvent like-UiO-66 (DES-UiO-66) composite, through in-situ forming strong hydrogen bonds directly between the MOF and cheap and safe choline chloride. The urea functionality was covalently introduced into the UiO-66-NH<sub>2</sub> through polymerization between the 2-aminoterephthalate linkers and 1,4-phenylene diisocyanate toward formation a new urea functionalized UiO-66-NH<sub>2</sub>, named here UiO-66-Urea. Then, PSM of UiO-66-Urea with choline chloride (ChCl) under thermal and solvent-free conditions resulted in in-situ formation of  $\text{ChCl}@\text{UiO-66-Urea}$ . The urea

installed onto the UiO-66-NH<sub>2</sub> by PSM, is used as hydrogen donor and the ChCl is used as hydrogen acceptor. As schematically presented in Scheme 1, the presence of urea groups and ChCl may induce strong hydrogen bond interactions between both as observed for the homogeneous ChCl-2Urea mixture [23,57]. UiO-66-NH<sub>2</sub> was selected due to its robustness, high surface area, and reproducible synthesis [21,58]. The node of UiO-66-NH<sub>2</sub> is a  $\text{Zr}_6\text{O}_4(\text{OH})_4$  cluster that comprises Lewis-acidic Zr(IV) sites which are settled in the framework as same as active sites of phosphotriesterase enzymes [59]. By such a design, a novel and bioinspired porous deep eutectic solvent like-MOF is constructed. The resulted organic-inorganic hybrid solid was then used for the one-pot three-component synthesis of 2-amino-4*H*-chromenes through reactions of aldehydes, malononitrile, and  $\alpha$ -naphthol or 4-hydroxycoumarin under environmentally-benign conditions. To the best of our knowledge, this is the first report on the synthesis and use of such DES/MOF or IL/MOF as heterogeneous catalyst for a multicomponent reaction.

## 2. Experimental section

### 2.1. Materials

Zirconium chloride ( $\text{ZrCl}_4$ , Sigma-Aldrich,  $\geq 99.5\%$ ), 2-aminoterephthalic acid (ACROS Organics, 99%), 1,4-phenylene diisocyanate (TCL Chemicals,  $> 98\%$ ), choline chloride (ChCl, Sigma-Aldrich,  $\geq 99\%$ ), *N,N'*-dimethylformamide (DMF, Merck,  $\geq 99.8\%$ ), 4-hydroxycoumarin (Sigma-Aldrich, 98%), 1-naphthol (Merck,  $\geq 99\%$ ), and other reagents were purchased from Merck and/or Sigma-Aldrich and used as received.

### 2.2. Characterization

Thermogravimetric analysis (TGA, Mettler Toledo) was measured under nitrogen atmosphere ( $T = 25\text{--}700\text{ }^\circ\text{C}$  with heating rate of  $10\text{ }^\circ\text{C}/\text{min}$ ).  $^1\text{H}$  NMR and  $^{13}\text{C}$  NMR spectra were recorded in a Bruker Advance 300 or 250 MHz (300 or 250 MHz for  $^1\text{H}$ , 62.9 MHz for  $^{13}\text{C}$ ) using deuterated DMSO as solvent. Powder X-ray diffraction (PXRD) data were collected on a Philips X'pert diffractometer using Cu K $\alpha$  radiation ( $\lambda = 1.5418\text{ \AA}$ ). The morphology and chemical composition of the samples were investigated by field emission scanning electron

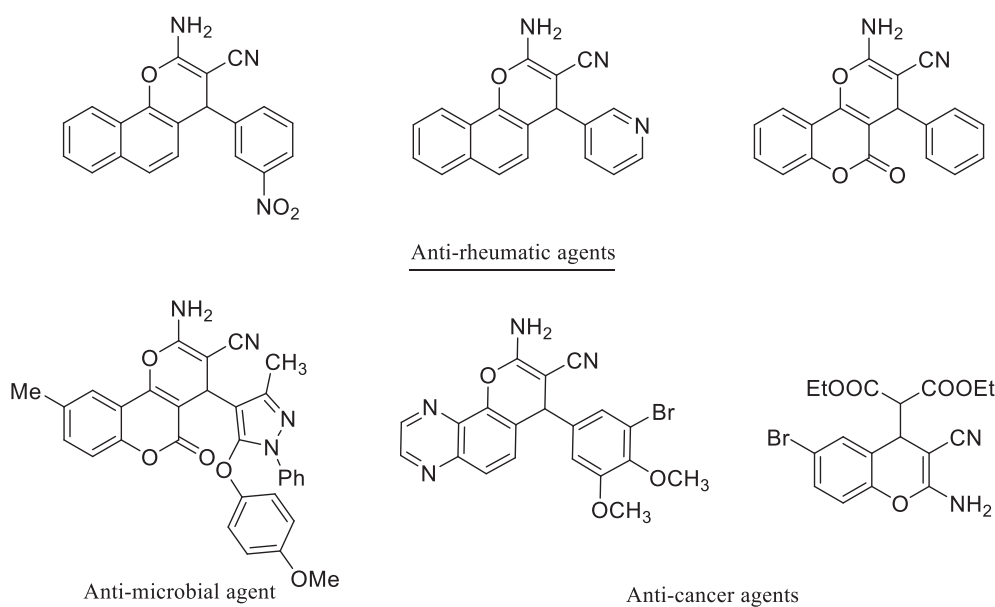
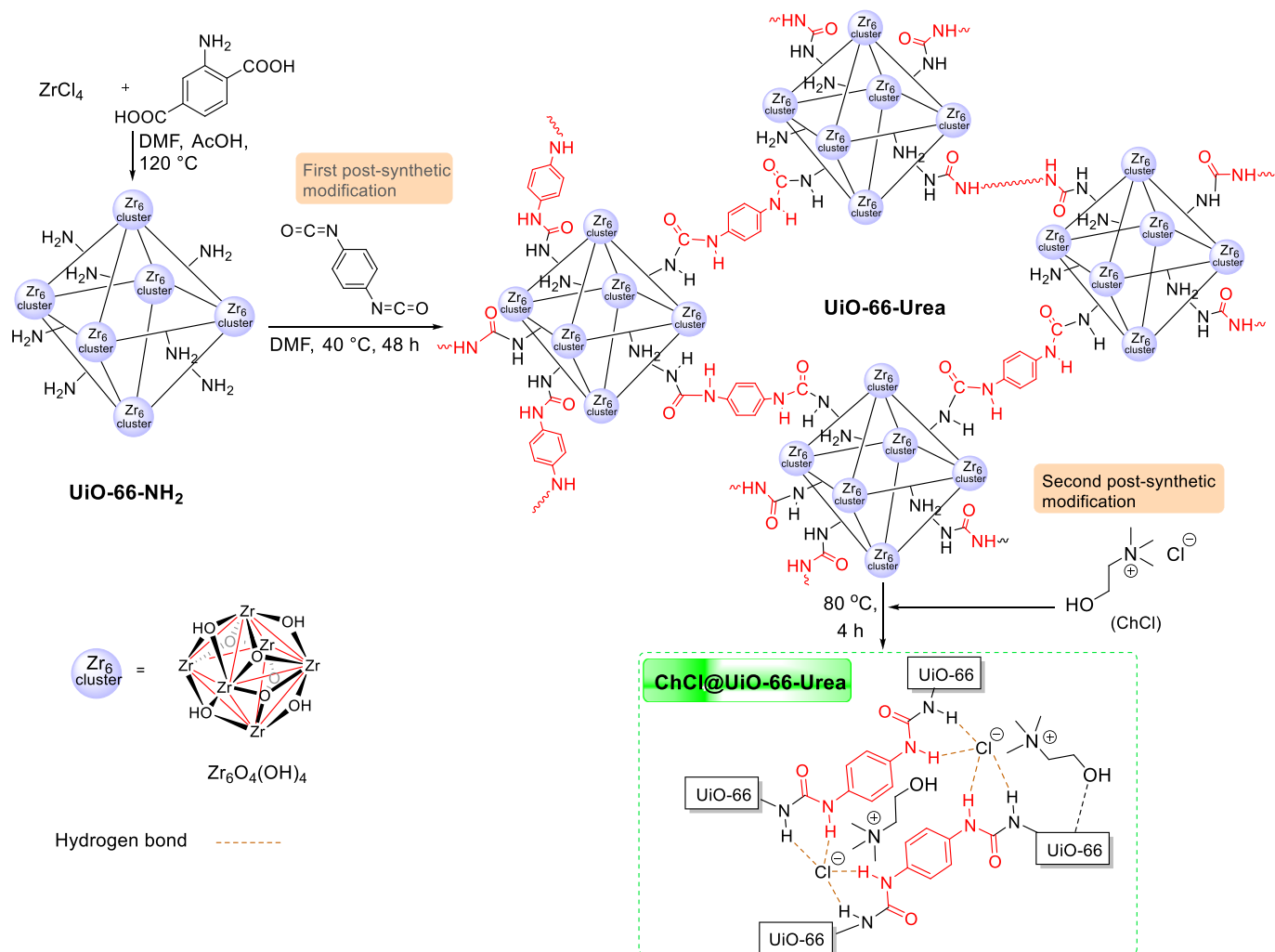


Fig. 1. Biological and pharmacological active 2-amino-4*H*-chromenes.



**Scheme 1.** Schematic representative of synthesis of ChCl@UiO-66-Urea.

microscopy (FE-SEM, MIRA3 TESCAN) equipped with an energy dispersive X-ray spectrometer (EDX). Nitrogen adsorption isotherms at 77 K were gained by using a volumetric adsorption analyze (Micromeritics TriStar II. 3020 Version 3.02). The Fourier-transformed infrared (FT-IR) spectra were obtained by a Perkin Elmer Spectrum-FTIR.

### 2.3. Synthesis of UiO-66-NH<sub>2</sub>

UiO-66-NH<sub>2</sub> was synthesized according to the previously reported procedure [58,60]; In a 250-mL round-bottom flask, ZrCl<sub>4</sub> (0.4 g, 1.7 mmol) in DMF (75 mL) was sonicated at 50–60 °C for 10 min, and acetic acid (2.85 mL) was added to the clear solution. A solution of 2-aminoterephthalic acid (0.311 g, 1.7 mmol) in DMF (25 mL) was then discharged to the earlier solution before being sonicated for additional 10 min. Next, water (0.125 mL, 0.007 mmol) was discharged to the resultant solution followed by sonication for 5 min. The flask was capped tightly and sonicated at –50 °C for 20 min and then heated at 120 °C for 24 h without stirring. After the time, the solution was cooled down to room temperature and the solid was collected by filtration, washed with DMF (3 times) and then ethanol (4 times). Lastly, the particulate was dried (90 °C, 3 h, under reduced pressure) to give the Zr<sub>6</sub>O<sub>4</sub>(OH)<sub>4</sub> (BDC-NH<sub>2</sub>)<sub>6</sub> MOF (580 mg). FT-IR (ATR, cm<sup>-1</sup>): 3469, 3359, 1657, 1573, 1494, 1434, 1383, 1336, 1258, 1157, 1096, 764, 664, 572, 476, 430.

### 2.4. Synthesis of urea covalently introduced into UiO-66-NH<sub>2</sub> (UiO-66-Urea)

The UiO-66-NH<sub>2</sub> (activated, 100 mg, 0.349 mmol NH<sub>2</sub>) in dry DMF (2.5 mL) was magnetically stirred for 5 min under N<sub>2</sub> atmosphere at room temperature. 1,4-phenylene diisocyanate (176 mg, 1.1 mmol) was dissolved in dry DMF (5 mL) and added to the suspension, while the mixture was stirred under N<sub>2</sub> atmosphere. The resultant mixture was heated at 40 °C and stirred for 48 h under N<sub>2</sub> condition. Finally, the reaction mixture was cooled down to room temperature and acetone was added and stirred for 60 min. After that, the particulate was isolated by centrifugation and washed several times with acetone and ethanol. The precipitate was soaked in acetone for 24 h and then collected by centrifugation. Lastly, the solid was dried at room temperature under reduced pressure, then at 80 °C for 12 h, and finally, at 130 °C for 4 h (Yield = 230 mg). FT-IR (ATR, cm<sup>-1</sup>): 3295, 1630, 1565, 1510, 1430, 1389, 1300, 1219, 1106, 1068, 1015, 823, 766, 664, 519, 480, 417.

### 2.5. Synthesis of deep eutectic solvent-like into UiO-66-NH<sub>2</sub> (ChCl@UiO-66-Urea)

The obtained UiO-66-Urea (50 mg) and ChCl (31 mg, 0.3 mmol) were added in a test tube and the mixture was magnetically stirred

for 4 h at 80 °C, before being cooled to room temperature. After that, a dark yellow solid was obtained. FT-IR (ATR,  $\text{cm}^{-1}$ ): 3293, 3024, 1630, 1557, 1508, 1434, 1406, 1382, 1298, 1258, 1080, 1013, 1006, 952, 865, 823, 767, 644, 518, 473, 416.

## 2.6. General procedure for the one-pot three-component synthesis of chromenes

A typical mixture of aldehyde (1 mmol), malononitrile (1 mmol), 4-hydroxycoumarin or  $\alpha$ -naphthol (1 mmol), and  $\text{ChCl@UiO-66-Urea}$  (10 mg) in a test tube was stirred magnetically under solvent-free condition at 80 °C for the indicated time (see Table 2). After the completion of the reaction, monitored by thin layer chromatography (TLC) using n-hexane/ethyl acetate (7:3 v/v), the organic compounds were dissolved in low amount of chloroform. Then, the MOF-based catalyst was isolated by centrifugation. After evaporation of the solvent, the residue was recrystallized from ethanol to afford the desired product. The products were characterized by physical and spectroscopic data (Melting point, FT-IR,  $^1\text{H}$  NMR, and  $^{13}\text{C}$  NMR) as given in supporting information (SI).

## 3. Result and discussion

### 3.1. $\text{ChCl@UiO-66-Urea}$ characterization

$\text{UiO-66-NH}_2$  was firstly synthesized starting from  $\text{ZrCl}_4$  and 2-aminoterephthalic acid via solvothermal condition according to the previously reported procedure [58,60]. Subsequently, the free amino groups were reacted with 1,4-phenylene diisocyanate at 40 °C under nitrogen atmosphere for 48 h to yield urea moieties which are covalently linked to  $\text{UiO-66-NH}_2$  (named  $\text{UiO-66-Urea}$ ) (Scheme 1). Further, post-synthetic modification of  $\text{UiO-66-Urea}$  with choline chloride ( $\text{ChCl}$ ) resulted in in-situ formation of a deep eutectic solvent, might be similar to  $\text{ChCl-2Urea}$  [23],  $[\text{Choline}]^+[\text{Cl}(\text{urea})_2]^-$ , into the  $\text{UiO-66-Urea}$  MOF (named  $\text{DES-UiO-66}$  or  $\text{ChCl@UiO-66-Urea}$ ), in which urea comes from  $\text{UiO-66-Urea}$  and can act as hydrogen-bond donor whereas  $\text{ChCl}$  can act as hydrogen-bond acceptor (Scheme 1).

The successful post-synthetic modifications can be initially assessed by IR spectroscopy. FT-IR spectra of  $\text{UiO-66-NH}_2$ ,  $\text{UiO-66-Urea}$ , and  $\text{ChCl@UiO-66-Urea}$  are shown in Fig. S1-S3. The peaks at 3469 and  $\sim 3360\text{ cm}^{-1}$  are assigned to asymmetric and symmetric vibrations of the amino groups in  $\text{UiO-66-NH}_2$  (Fig. S1). The peaks appeared at 1657, 1573, 1494, 1383, and  $1258\text{ cm}^{-1}$  are attributed respectively to the stretching modes of  $\text{C=O}$ ,  $\text{O-C=O}$  (asymmetric carboxylate),  $\text{C=C}$ ,  $\text{O-C=O}$  (symmetric carboxylate), and  $\text{C}_{\text{aromatic}}-\text{N}$  bonds [58,61]. The observed intense peak at  $\sim 764\text{ cm}^{-1}$  is ascribed to N-H wagging band [62]. Further peaks at lower frequencies between 475 and  $664\text{ cm}^{-1}$  are related to -OH and -CH bending and Zr-O vibrations. The band centered at  $664\text{ cm}^{-1}$  is assigned to stretching mode of  $\mu_3-\text{O}$  in  $\text{Zr-O-Zr}$  [20,62]. In IR spectrum of  $\text{UiO-66-Urea}$  (Fig. S2 in the Supporting Information), the complete removal of the stretching band of  $-\text{N}=\text{C}=\text{O}$  of the isocyanate at  $\sim 2250\text{ cm}^{-1}$  was associated with appearance of the new characteristic stretching bands of the urea moiety, N-H at  $3295\text{ cm}^{-1}$ ,  $\text{C=O}$  at  $1630\text{ cm}^{-1}$ , and N-C-N at  $1300\text{ cm}^{-1}$  [63]. At the same time, the bands related to the N-H-stretching vibrations of the amino group are clearly diminished. These data confirm the urea formation and its linkage to the MOF, namely,  $\text{UiO-66-Urea}$ . After the last post-synthetic modification of  $\text{UiO-66-Urea}$  with choline chloride, the new characteristic bands of the  $\text{ChCl}$  are observed at 3024, 1080, 952, and  $865\text{ cm}^{-1}$ , which are respectively related to the asymmetric bending -OH, rocking  $\text{CH}_2$ , asymmetric stretching of CCO, and stretching  $\text{N-CH}_3$  [64] (Fig. S3). Additionally, the absorption band of  $\text{UiO-66-Urea}$  at  $3295\text{ cm}^{-1}$  is moved to the lower wavenumber of  $3293\text{ cm}^{-1}$  and become broader as shown in the Fig. S3. It could be due to the strong hydrogen bonds formed between  $\text{UiO-66-Urea}$  and  $\text{ChCl}$ . These results suggest the successful  $\text{UiO-66-NH}_2$  modifications toward formation of the  $\text{ChCl@UiO-66-Urea}$ .

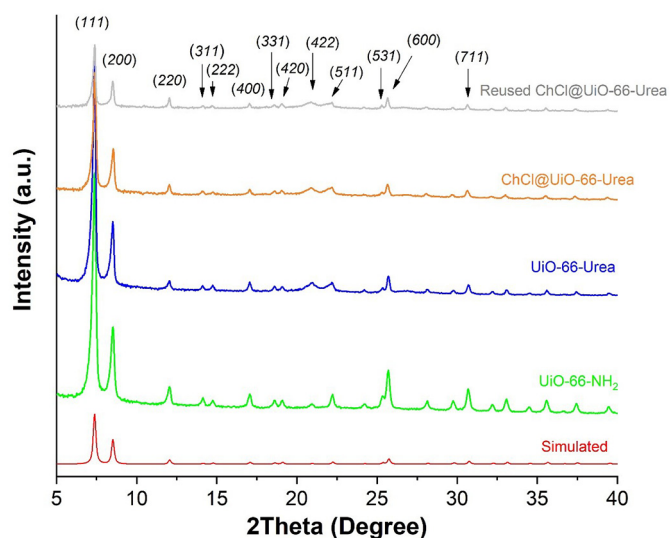


Fig. 2. Large-angle XRD patterns from bottom to up:  $\text{UiO-66-NH}_2$  (simulated, red), as-synthesized  $\text{UiO-66-NH}_2$  (green),  $\text{UiO-66-Urea}$  (blue),  $\text{ChCl@UiO-66-Urea}$  (brown), and reused  $\text{ChCl@UiO-66-Urea}$  (gray).

Subsequently, the crystallinity of as-synthesized  $\text{UiO-66-NH}_2$ ,  $\text{UiO-66-Urea}$ , and  $\text{ChCl@UiO-66-Urea}$  were evaluated by powder X-ray diffractometer (PXRD). As shown in Fig. 2, all of the XRD patterns clearly showed the reflection peaks of  $2\theta = 7.36, 8.50, 12.06, 14.12, 14.77, 17.06, 18.59, 19.08, 20.96, 22.20, 25.35, 25.69,$  and  $30.68$ , which corresponded, respectively, to (111), (200), (220), (311), (222), (400), (331), (420), (422), (511), (531), (600), and (711) Bragg planes as the same those of the simulated and reported  $\text{UiO-66-NH}_2$  [20,58,59,61]. This result was proved that these three MOF structures are the same and the pristine  $\text{UiO-66-NH}_2$  remained obviously intact after the post-synthetic modifications.

Besides, the morphology, shape, and size of  $\text{UiO-66-NH}_2$ ,  $\text{UiO-66-Urea}$ , and  $\text{ChCl@UiO-66-Urea}$  were assessed by SEM (Fig. 3a-i). The images showed that the pristine  $\text{UiO-66-NH}_2$  particles have octahedral morphology in the size range of 90 to 200 nm (Fig. 3a-c). In addition, as given in the Fig. 3d-i, the primary MOF particles are remained unchanged after the modification procedures. Further, the polymerization of MOF particles through reacting with the diisocyanate in the second process, and subsequently, their integration with  $\text{ChCl}$ , yielding the  $\text{ChCl@UiO-66-Urea}$ , deep eutectic solvent over the  $\text{UiO-66-NH}_2$ , are noticeable in the Fig. 3d-i. Next, energy dispersive X-ray (EDX) analysis of the  $\text{ChCl@UiO-66-Urea}$  revealed the presence of the elemental composition of C (46.26 wt%), N (23.23 wt%), O (19.71 wt%), Zr (4.79 wt%), and particularly Cl (6.01 wt%) in the material, approving the successful post-synthetic modifications (Fig. S4). Moreover, the elemental mapping images of the respective MOF confirmed that the all elements (notably Cl) were distributed homogeneously in the whole framework (Fig. 4).

Nitrogen adsorption-desorption measurements indicated that  $\text{ChCl@UiO-66-Urea}$  is prominently porous with a Brunauer-Emmett-Teller (BET) surface area of  $350\text{ m}^2\text{ g}^{-1}$  and a total pore volume of  $0.26\text{ cm}^3\text{ g}^{-1}$  (Fig. 5). The observed decrease in BET surface area from  $\text{UiO-66-NH}_2$  to  $\text{ChCl@UiO-66-Urea}$ , respectively, from  $850\text{ m}^2\text{ g}^{-1}$  of  $350\text{ m}^2\text{ g}^{-1}$ , is due to the formation of urea linkages and their merging with  $\text{ChCl}$  toward synthesis of the  $\text{DES-UiO-66}$ . Furthermore, the isotherm curve of the  $\text{DES-UiO-66}$  is a typical type I shape which is representative of a microporous material.

Porosity distribution calculated from nitrogen sorption data by using DFT model confirmed the presence of micropores (1–1.2 and  $\sim 1.5\text{ nm}$ ) in the framework (Fig. 6).

Further, thermogravimetric analysis (TGA) was employed to evaluate the thermal stability of MOFs. TG curves of  $\text{UiO-66-NH}_2$ ,  $\text{UiO-66-}$

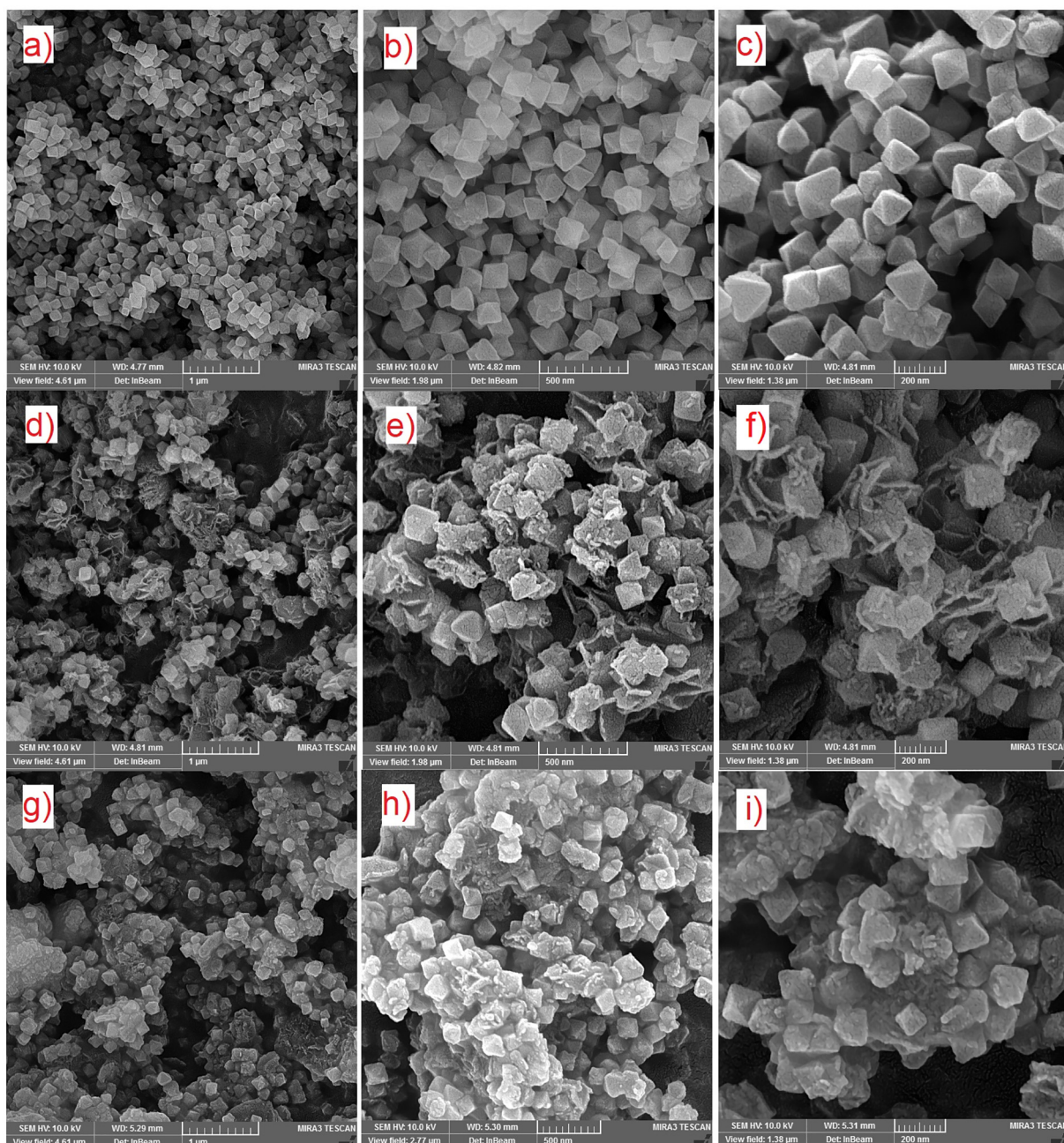


Fig. 3. SEM images of UiO-66-NH<sub>2</sub> (a-c), UiO-66-Urea (d-f), and ChCl@UiO-66-Urea (g-i).

Urea, and ChCl@UiO-66-Urea are presented in Fig. 7. For the all samples, the initial mass loss before 200 °C was due to the elimination of physically adsorbed water and solvents trapped in the pores of the MOFs. For the UiO-66-NH<sub>2</sub>, mass loss (~19 wt%) between 200 and 360 °C was due to dihydroxylation of the [Zr<sub>6</sub>O<sub>4</sub>(OH)<sub>4</sub>]<sup>12+</sup> nodes [60,65]. Mass loss above 380 °C was related to the thermal decomposition of 2-aminoterephthalic acid ligands and the breakdown of the UiO-66-NH<sub>2</sub>, which finally resulted in the formation of solid ZrO<sub>2</sub> [58]. Comparably, the UiO-66-Urea showed a mass loss ~36 wt% between 200 and 380 °C which might be due to the dehydroxylation of Zr<sub>6</sub> nodes associated with the cleavage of the installed urea moieties. Further, the ChCl@UiO-66-Urea exhibited two distinct mass loss regions in the temperature ranges of 200–340 °C (200 to 280 °C and 280 to 340 °C). Mass loss of ~16 wt% in the region of 200 to 280 °C, might be due to the dehydroxylation of Zr<sub>6</sub> nodes, and a major mass loss of ~42 wt% in the region

of 280 to 340 °C, might be due to the decomposition of the DES components [64] and the beginning cleavage of the MOF framework. This thermal stability of ChCl@UiO-66-Urea (around 300 °C) is promising for its use as a heterogeneous catalyst.

### 3.2. Catalytic reactions for the synthesis of chromenes

As part of our efforts in developing MOF catalysis [6,58,61], we decided to examine the catalytic performance of ChCl@UiO-66-Urea for the multicomponent synthesis of chromenes. Thus, the reaction between benzaldehyde, malononitrile, and  $\alpha$ -naphthol was chosen as a model reaction and optimized by the variation of temperature, catalyst loading, and reaction medium as the results shown in Table 1. Initially, the effect of reaction temperature on the yield of the reaction toward synthesis of 2-amino-4-phenyl-4H-benzo[h]chromene-3-carbonitrile

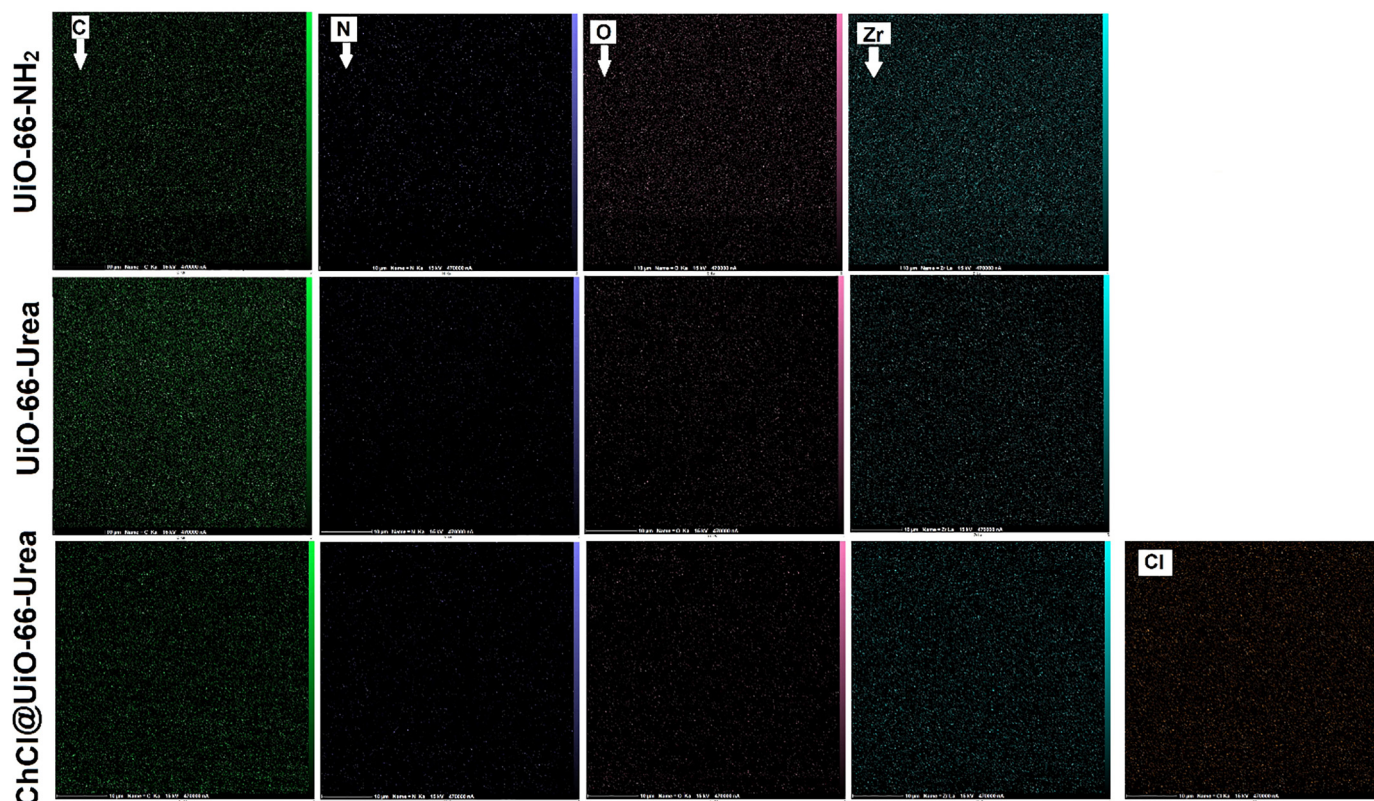


Fig. 4. Energy dispersive X-ray spectroscopy (EDX) elemental mapping images of UiO-66-NH<sub>2</sub>, UiO-66-Urea, and ChCl@UiO-66-Urea.

was investigated (Table 1, entries 1–3). When the reaction was carried out under solvent-free condition at 50 °C in the presence of the catalyst, the product yield reached 41% (Entry 1). With the increasing temperature from 50 °C to 80 °C, the observed yield was dramatically increased to 92% (Entry 2) and the highest yield obtained at this temperature after 3 h. However, after the further increase of reaction temperature to 100 °C, the product yield was slightly decreased to 91% (Entry 3). Next, the effect of the catalyst loading (5–15 mg) on the yield of the product was examined (Table 1, entry 2 vs. entries 4 & 5). As shown in Entry 4, in low amount of the catalyst, the yield of product was

obviously decreased. The highest yield was achieved in the amount of catalyst of 10 mg (Entry 2). With the increasing the catalyst loading from 10 mg to 15 mg, no significant improvement in the product yield was obtained (Entry 5). Therefore, in view of the less use of the catalyst, 10 mg of the ChCl@UiO-66-Urea was chosen as the best amount of catalyst. Then, the catalytic activity of ChCl@UiO-66-Urea was tested under identical conditions in different reaction media including solvent-free or solvent conditions such as ethanol, ethanol/water, and ethyl acetate, as the results given in the Table 1 (Entry 2 vs. Entries 7–9). As shown in the Table 1, the highest yield was reached under solvent-free condition at

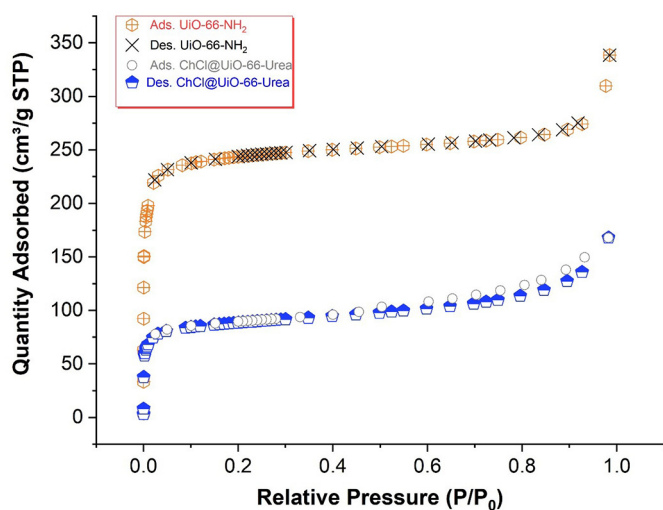


Fig. 5. N<sub>2</sub> adsorption-desorption isotherms of UiO-66-NH<sub>2</sub> (top) and ChCl@UiO-66-Urea (bottom) at 77 K.

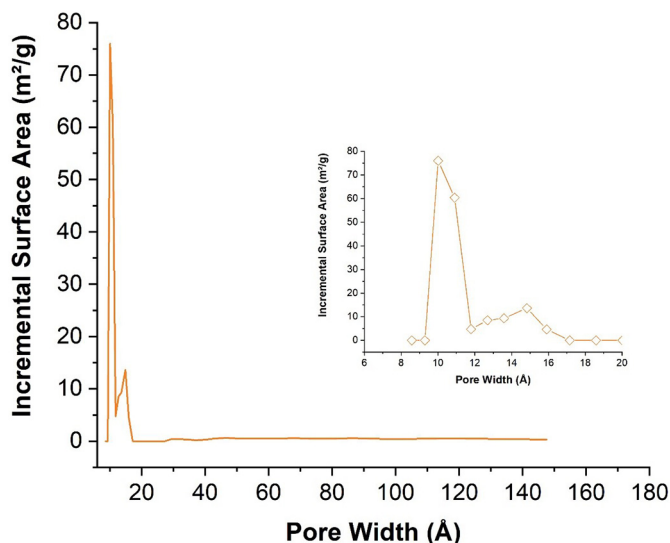


Fig. 6. DFT pore size distribution for the ChCl@UiO-66-Urea sample.

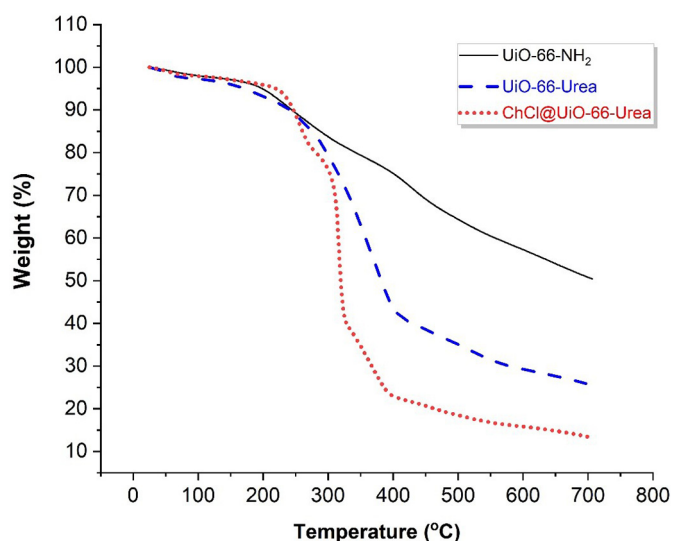


Fig. 7. TG curves of UiO-66-NH<sub>2</sub> (top), UiO-66-Urea (middle), and ChCl@UiO-66-Urea (bottom).

80 °C after 3 h (Entry 2). To further understand the active sites of the MOF, UiO-66-NH<sub>2</sub> was examined as catalyst for the model reaction under the optimal reaction conditions. The observed yield was 32% with UiO-66-NH<sub>2</sub> (Entry 10, Table 1) which was comparatively lower than using ChCl@UiO-66-Urea as catalyst. The reaction under similar conditions in the presence of UiO-66 afforded 25% yield of the product (Entry 11, Table 2). The use of UiO-66-Urea as catalyst resulted in 46% yield of the product under identical conditions (Entry 12). Also, ChCl as catalyst produced a much lower yield compared to that of the ChCl@UiO-66-Urea (Entry 13). When homogenous ChCl-2urea, mixing urea and ChCl (ratio 2:1) at 80 °C for 3 h, was used as the catalyst, the product yield was remarkably increased to 69% (Entry 14), but is still comparatively lower than using ChCl@UiO-66-Urea as catalyst. To

further study the role of Zr<sub>6</sub>-nodes on the catalytic activity of ChCl@UiO-66-Urea, ZrCl<sub>4</sub> as the Zr-node precursor was also examined as catalyst for the model reaction (Entry 15), which resulted in 24% yield of the product. These experiments evidently reveal that the catalytic activity of ChCl@UiO-66-Urea comes from its ChCl@Urea moiety, although the Lewis acid Zr(IV) nodes can serve as active sites as well. In addition, the experiments further confirmed synergistic effects between ChCl and UiO-66-Urea interactions which resulted in the enhancement of catalytic activity of ChCl@UiO-66-Urea compared to the others (Table 1, entries 10–14).

Next, under the optimized reaction conditions, the substrate scope of the multicomponent reactions was checked. Therefore, several aryl aldehydes were verified under the optimized reaction conditions (Table 2). As shown in Table 2, the aldehydes with a wide range of electron-donating and electron-withdrawing substituents reacting with  $\alpha$ -naphthol (or 4-hydroxycoumarin instead of  $\alpha$ -naphthol) all afforded the desired products in good to excellent yields. In addition, electron-poor aromatic aldehydes provided the corresponding products in slightly higher yield and/or faster reaction time (Table 2). Besides, the steric hindrance effect of *ortho*-chloro groups showed no significant influence on the reaction efficiency (Table 2, entries 3 and 9).

According to our experimental results and previously reported procedures [47–49], the proposed mechanism for the one-pot three-component reactions was represented in Scheme 2. Accordingly, the process is initiated with the activation of aldehyde and malononitrile with porous ChCl@UiO-66-Urea catalyst due to Lewis acidity of Zr-MOF [21,58], Brønsted basicity and hydrogen bonding ability of urea groups [23,66,67]. The hydroxyl group of choline also may act as a hydrogen bond catalyst [68] for the reaction. In addition, the impregnation of UiO-66-Urea with choline chloride greatly facilitates the contact between the ChCl@UiO-66-Urea and starting materials, due to in-situ formation a deep eutectic or low-melting mixture [23,67]. Subsequently, the catalytic cycle is most probably continued with the Knoevenagel condensation reaction between the activated aldehyde and malononitrile to give the intermediate **I** (Knoevenagel reaction). The next step involves the regioselective nucleophilic addition of  $\alpha$ -naphthol/4-hydroxycoumarin (C-addition) to the intermediate **I** to form the intermediate **II** (Michael addition). Finally, the intermediate

Table 1  
Optimization of the reaction conditions for the three-component synthesis of 2-amino-4H-chromenes.<sup>a</sup>

Entry	Catalyst	Catalyst amount (mg)	Time (h)	T(°C)	Solvent	Yield (%) <sup>b</sup>
1	ChCl@UiO-66-Urea	10	3	50	Solvent-free	41
2	ChCl@UiO-66-Urea	10	3	80	Solvent-free	92
3	ChCl@UiO-66-Urea	10	3	100	Solvent-free	91
4	ChCl@UiO-66-Urea	5	3	80	Solvent-free	60
5	ChCl@UiO-66-Urea	15	3	80	Solvent-free	92
7	ChCl@UiO-66-Urea	10	5	80	EtOH	72
8	ChCl@UiO-66-Urea	10	5	80	EtOH/H <sub>2</sub> O	59
9	ChCl@UiO-66-Urea	10	5	80	EtOAc	41
10	UiO-66-NH <sub>2</sub>	10	3	80	Solvent-free	32
11	UiO-66	10	3	80	Solvent-free	25
12	UiO-66-Urea	10	3	80	Solvent-free	46
13	ChCl	10	3	80	Solvent-free	18
14	ChCl-urea	10	3	80	Solvent-free	69
15	ZrCl <sub>4</sub>	8	3	80	Solvent-free	24

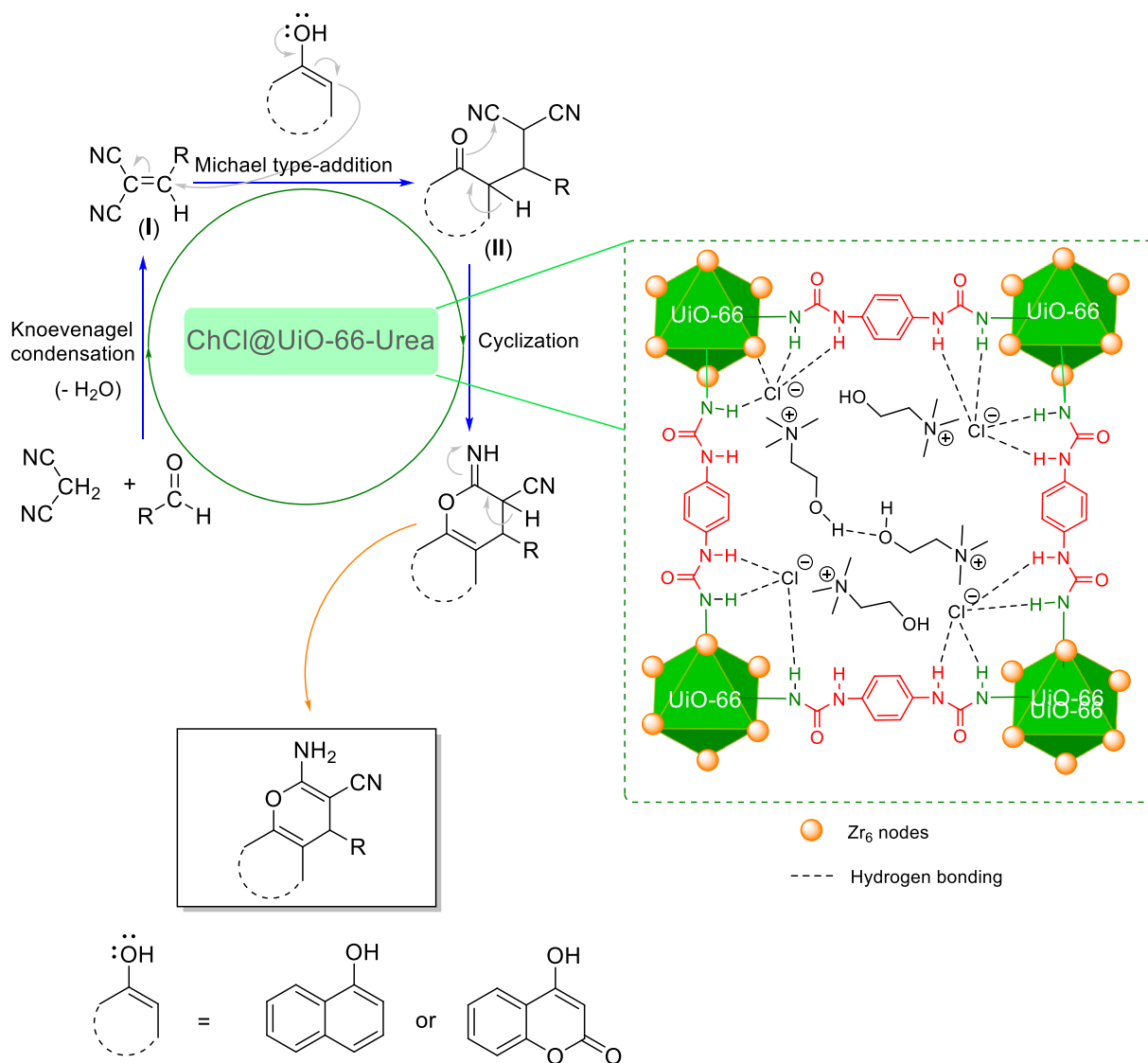
<sup>a</sup> Reaction conditions: benzaldehyde (1 mmol), malononitrile (1 mmol),  $\alpha$ -naphthol (1 mmol), and catalyst.

<sup>b</sup> Yields refer to isolated and purified products.

**Table 2**One-pot three-component synthesis of 2-amino-4H-chromene derivatives using  $\text{ChCl@UiO-66-Urea}$  catalyst.<sup>a</sup>

Entry	Product	Time (h)/ Yield (%) <sup>b</sup>	m.p. (°C) <sup>c</sup>	Entry	Product	Time (h)/ Yield (%) <sup>b</sup>	m.p. (°C) <sup>c</sup>
1		3/92	213-215	8		3/91	245-247
2		3/91	240-242	9		4.5/85	270-273
3		4/89	245-247	10		3.5/91	266-270
4		2.5/91	217-219	11		3/92	260-262
5		2.5/92	218-220	12		4/87	247-249
6		3/92	180-183	13		4/84	231-232
7		4.5/91	203-205				

<sup>a</sup> Reaction conditions: aromatic aldehyde (1 mmol), malononitrile (1 mmol),  $\alpha$ -naphthol/4-hydroxycoumarin (1 mmol), and  $\text{ChCl@UiO-66-Urea}$  (10 mg) under solvent-free condition at 80 °C.<sup>b</sup> Yields refer to isolated and purified products.<sup>c</sup> Observed melting points.



**Scheme 2.** Proposed mechanism for the three-component synthesis of chromenes using ChCl@UiO-66-Urea as the catalyst.

**II** undergoes intramolecular ring closure to produce the corresponding chromene (Cyclization) and the regenerated catalyst is simultaneously used in the next cycle.

Further, the stability and reusability of ChCl@UiO-66-Urea were checked using the model reaction. After the completion of the reaction, the catalyst was removed from the reaction mixture with chloroform and dried at 90 °C under vacuum. The catalyst was reused in next cycle

without significant loss in its catalytic efficiency. As exhibited in Fig. S5, the decrease in efficiency of ChCl@UiO-66-Urea catalyst after the third and fifth cycles were 4 and 7%, respectively. However, the catalytic activity was still high of 85% even after five times use. To further check the stability of the catalyst, the reused ChCl@UiO-66-Urea was then characterized by PXRD, FT-IR, and EDX elemental analysis. Accordingly, the PXRD of the reused catalyst was indicated that its structure was

**Table 3**  
Comparison of the catalytic activity of ChCl@UiO-66-Urea with catalysts reported for the one-pot three-component reaction of benzaldehydes, malononitrile, and  $\alpha$ -naphthol.

Entry	Catalyst (amount)	Solvent	Temperature (°C)	Time (h)	Yield (%)	Ref.
1	Nanostructured diphosphate Na <sub>2</sub> CaP <sub>2</sub> O <sub>7</sub> (DIPH) (0.3 g)	H <sub>2</sub> O	Reflux	4	90	44
2	Sodium-modified hydroxyapatite (100 mg)	H <sub>2</sub> O	Reflux	3	96	45
3	Silica-supported piperazine (185 mg) (for 4-chlorobenzaldehyde)	CHCl <sub>3</sub>	Reflux	7	74	46
4	Alkylaminopyridine-grafted on HY Zeolite (Z-HY@SiO <sub>2</sub> -Pr-Py) (30 mg)	Solvent-free	100	80 min	90	47
5	H <sub>14</sub> [NaP <sub>3</sub> W <sub>30</sub> O <sub>110</sub> ] (30 mg)	H <sub>2</sub> O	Reflux	3	91	48
6	2D-hexagonal mesoporous material functionalized with a triazine moiety (40 mg) (for 4-chlorobenzaldehyde)	Solvent-free	110	4	90	49
7	ChCl@UiO-66-Urea (10 mg)	Solvent-free	80	3	92	This work

maintained compared to the fresh one (Fig. 2). In addition, the FT-IR of the reused catalyst was almost the same as the fresh one (Fig. S6). However, EDX analysis of ChCl@UiO-66-Urea after fifth cycle (Fig. S7) showed the leaching of ChCl under the optimized reaction condition (~5% leaching in comparison to the fresh one, Fig. S4). These results lay out that the prepared ChCl@UiO-66-Urea has the potential to be used as a recyclable catalyst under the reaction conditions. The results of the present work were compared with those of the reported catalytic systems in the reaction of benzaldehyde, malononitrile, and  $\alpha$ -naphthol for the three-component synthesis of the corresponding chromene as illustrated in Table 3. As shown in the Table 3, the respective catalyst showed higher or comparable performance to some previously reported values.

#### 4. Conclusion

In this work, we proposed and developed an approach based on the coating of UiO-66-Urea solid with choline chloride (ChCl) to form *in situ* a deep eutectic mixture on the MOF surface, namely, ChCl@UiO-66-Urea. UiO-66-Urea was prepared through the reaction between the 2-aminoterephthalic linkers of the UiO-66-NH<sub>2</sub> and 1,4-phenylene diisocyanate in DMF solvent under inert atmosphere at 40 °C. After the deposition of ChCl on the UiO-66-Urea, not only the porosity of the MOF was mainly maintained, but also the catalytic activity of the MOF was impressively improved. The 2-amino-4H-chromenes were achieved in good to excellent yields through reactions between aromatic aldehydes, malononitrile, and  $\alpha$ -naphthol or 4-hydroxycoumarin under solvent-free condition at 80 °C using the low amount of the catalyst. Lewis acidity of Zr<sub>6</sub>-node, Brønsted basicity and hydrogen bonding capability of urea groups catalyzed the reactions. The presence of ChCl on the MOF surface may facilitate the contact between the solid catalyst and the reagents. Notably, the results showed that the hybrid catalyst performed almost better than the other previously reported catalysts. These data of the work can then be used to improve the catalytic behavior of MOFs. Furthermore, the work can open doors for future potential of such hybrid-based MOFs as new catalysts for a wide range of multi-component reactions in green chemistry concepts.

#### CRedit authorship contribution statement

**Mohadeseh Akbarian:** Investigation, Visualization, Formal analysis; **Esmael Sanchooli:** Validation, Investigation, Resources, Methodology, Funding acquisition, Co-supervision; **Ali Reza Oveisi:** Supervision, Project administration, Writing - review & editing; **Saba Daliran:** Conceptualization, Formal analysis, Visualization, Writing - original draft.

#### Declaration of Competing Interest

The authors declare that they have no known competing financial interests or personal relationships that could have appeared to influence the work reported in this paper.

#### Acknowledgment

This work was financed from the University of Zabol and is gratefully acknowledged (Grant NO.: UOZ-GR-9517-122 & UOZ-GR-9719-36).

#### Appendix A. Supplementary data

Supplementary data to this article can be found online at <https://doi.org/10.1016/j.molliq.2020.115228>.

#### References

[1] V. Pascanu, G. González Miera, A.K. Inge, B. Martín-Matute, Metal-organic frameworks as catalysts for organic synthesis: a critical perspective, *J. Am. Chem. Soc.* 141 (2019) 7223–7234.

[2] A. Bavykina, N. Kolobov, I.S. Khan, J.A. Bau, A. Ramirez, J. Gascon, Metal-organic frameworks in heterogeneous catalysis: recent progress, new trends, and future perspectives, *Chem. Rev.* 120 (2020) 8468–8535.

[3] A. Dhakshinamoorthy, A.M. Asiri, H. Garcia, 2D metal-organic frameworks as multi-functional materials in heterogeneous catalysis and electro/photocatalysis, *Adv. Mater.* 31 (2019) 1900617.

[4] A. Dhakshinamoorthy, A.M. Asiri, H. Garcia, Metal-organic frameworks as multi-functional solid catalysts, *Trends Chem.* 2 (2020) 454–466.

[5] A. Dhakshinamoorthy, S. Navalon, A.M. Asiri, H. Garcia, Metal organic frameworks as solid catalysts for liquid-phase continuous flow reactions, *Chem. Commun.* 56 (2020) 26–45.

[6] S. Oudi, A.R. Oveisi, S. Daliran, M. Khajeh, E. Teymouri, Brønsted-Lewis dual acid sites in a chromium-based metal-organic framework for cooperative catalysis: highly efficient synthesis of quinazolin-(4H)-1-one derivatives, *J. Colloid Interface Sci.* 561 (2020) 782–792.

[7] H. Alamgholiloo, S. Zhang, A. Ahadi, S. Rostamnia, R. Banaei, Z. Li, X. Liu, M. Shokouhimehr, Synthesis of bimetallic 4-PySI-Pd/Cu(BDC) via open metal site Cu-MOF: effect of metal and support of Pd/Cu-MOFs in H<sub>2</sub> generation from formic acid, *Mol. Catal.* 467 (2019) 30–37.

[8] A. Dhakshinamoorthy, A.M. Asiri, M. Alvaro, H. Garcia, Metal organic frameworks as catalysts in solvent-free or ionic liquid assisted conditions, *Green Chem.* 20 (2018) 86–107.

[9] A. Dhakshinamoorthy, H. Garcia, Metal-organic frameworks as solid catalysts for the synthesis of nitrogen-containing heterocycles, *Chem. Soc. Rev.* 43 (2014) 5750–5765.

[10] A. Dhakshinamoorthy, Z. Li, H. Garcia, Catalysis and photocatalysis by metal organic frameworks, *Chem. Soc. Rev.* 47 (2018) 8134–8172.

[11] D. Wang, Y. Pan, L. Xu, Z. Li, PdAu@MIL-100(Fe) cooperatively catalyze tandem reactions between amines and alcohols for efficient N-alkyl amines syntheses under visible light, *J. Catal.* 361 (2018) 248–254.

[12] H. Li, K. Wang, Y. Sun, C.T. Lollar, J. Li, H.-C. Zhou, Recent advances in gas storage and separation using metal-organic frameworks, *Mater. Today* 21 (2018) 108–121.

[13] L.E. Kreno, K. Leong, O.K. Farha, M. Allendorf, R.P. Van Duyne, J.T. Hupp, Metal-organic framework materials as chemical sensors, *Chem. Rev.* 112 (2012) 1105–1125.

[14] L. Latifi, S. Sohrabnezhad, Drug delivery by micro and meso metal-organic frameworks, *Polyhedron* 180 (2020) 114321.

[15] I. Abánades Lázaro, R.S. Forgan, Application of zirconium MOFs in drug delivery and biomedicine, *Coord. Chem. Rev.* 380 (2019) 230–259.

[16] T. Islamoglu, Z. Chen, M.C. Wasson, C.T. Buru, K.O. Kirlikovali, U. Afrin, M.R. Mian, O.K. Farha, Metal-organic frameworks against toxic chemicals, *Chem. Rev.* 120 (2020) 8130–8160.

[17] P. Deria, J.E. Mondloch, O. Karagiardi, W. Bury, J.T. Hupp, O.K. Farha, Beyond post-synthetic modification: evolution of metal-organic frameworks via building block replacement, *Chem. Soc. Rev.* 43 (2014) 5896–5912.

[18] S.M. Cohen, The Postsynthetic renaissance in porous solids, *J. Am. Chem. Soc.* 139 (2017) 2855–2863.

[19] L.R. Redfern, M. Ducamp, M.C. Wasson, L. Robison, F.A. Son, F.-X. Coudert, O.K. Farha, Isolating the role of the node-linker bond in the compression of UiO-66 metal-organic frameworks, *Chem. Mater.* 32 (2020) 5864–5871.

[20] J.H. Cavka, S. Jakobsen, U. Olsbye, N. Guillou, C. Lamberti, S. Bordiga, K.P. Lillerud, A new zirconium inorganic building brick forming metal organic frameworks with exceptional stability, *J. Am. Chem. Soc.* 130 (2008) 13850–13851.

[21] A. Dhakshinamoorthy, A. Santiago-Portillo, A.M. Asiri, H. Garcia, Engineering UiO-66 metal organic framework for heterogeneous catalysis, *ChemCatChem* 11 (2019) 899–923.

[22] B. Wang, L. Qin, T. Mu, Z. Xue, G. Gao, Are ionic liquids chemically stable? *Chem. Rev.* 117 (2017) 7113–7131.

[23] E.L. Smith, A.P. Abbott, K.S. Ryder, Deep eutectic solvents (DESs) and their applications, *Chem. Rev.* 114 (2014) 11060–11082.

[24] F.P. Kinik, A. Uzun, S. Keskin, Ionic liquid/metal-organic framework composites: from synthesis to applications, *ChemSusChem* 10 (2017) 2842–2863.

[25] M. Costa Gomes, L. Pison, C. Červinka, A. Padua, Porous ionic liquids or liquid metal-organic frameworks? *Angew. Chem. Int. Ed.* 57 (2018) 11909–11912.

[26] Q.-x. Luo, B.-w. An, M. Ji, J. Zhang, Hybridization of metal-organic frameworks and task-specific ionic liquids: fundamentals and challenges, *Mater. Chem. Front.* 2 (2018) 219–234.

[27] M. Zeeshan, V. Nozari, M.B. Yagci, T. Isik, U. Unal, V. Ortalan, S. Keskin, A. Uzun, Core-shell type ionic liquid/metal organic framework composite: an exceptionally high CO<sub>2</sub>/CH<sub>4</sub> selectivity, *J. Am. Chem. Soc.* 140 (2018) 10113–10116.

[28] X. Xia, G. Hu, W. Li, S. Li, Understanding reduced CO<sub>2</sub> uptake of ionic liquid/metal-organic framework (IL/MOF) composites, *ACS Appl. Nano Mater.* 2 (2019) 6022–6029.

[29] E.S. Larrea, R. Fernández de Luis, A. Fidalgo-Marijuan, E.M. Maya, M. Iglesias, M.I. Arriortua, Study of the versatility of CuBTC@IL-derived materials for heterogeneous catalysis, *CrystEngComm* 22 (2020) 2904–2913.

[30] N.M. Sabry, H.M. Mohamed, E.S.A.E.H. Khattab, S.S. Motlaq, A.M. El-Agrody, Synthesis of 4H-chromene, coumarin, 12H-chromeno[2,3-d]pyrimidine derivatives and some of their antimicrobial and cytotoxicity activities, *Eur. J. Med. Chem.* 46 (2011) 765–772.

[31] W. Kemnitzer, J. Drewe, S. Jiang, H. Zhang, C. Crogan-Grundty, D. Labreque, M. Bubenick, G. Attardo, R. Denis, S. Lamothe, H. Gourdeau, B. Tseng, S. Kasibhatla, S.X. Cai, Discovery of 4-Aryl-4H-chromenes as a new series of apoptosis inducers using a cell- and caspase-based high throughput screening assay. 4. Structure-activity relationships of N-alkyl substituted pyrrole fused at the 7,8-positions, *J. Med. Chem.* 51 (2008) 417–423.

- [32] E.F. Martin, A.T. Mbaveng, M.H. de Moraes, V. Kuete, M.W. Biavatti, M. Steindel, T. Efferth, L.P. Sandjo, Prospecting for cytotoxic and antiprotozoal 4-aryl-4H-chromenes and 10-aryldihydropyran[2,3-f]chromenes, *Arch. Pharm.* 351 (2018) 1800100.
- [33] M.N. Semenova, D.V. Tsyganov, O.R. Malyshev, O.V. Ershov, I.N. Bardasov, R.V. Semenov, A.S. Kiselyov, V.V. Semenov, Comparative in vivo evaluation of polyalkoxy substituted 4H-chromenes and oxa-podophyllotoxins as microtubule destabilizing agents in the phenotypic sea urchin embryo assay, *Bioorg. Med. Chem. Lett.* 24 (2014) 3914–3918.
- [34] S.A. Patil, R. Patil, L.M. Pfeffer, D.D. Miller, Chromenes: potential new chemotherapeutic agents for cancer, *Future Med. Chem.* 5 (2013) 1647–1660.
- [35] C.W. Smith, J.M. Bailey, M.E.J. Billingham, S. Chandrasekhar, C.P. Dell, A.K. Harvey, C.A. Hicks, A.E. Kingston, G.N. Wishart, The anti-rheumatic potential of a series of 2,4-di-substituted-4H-naphtho[1,2-b]pyran-3-carbonitriles, *Bioorg. Med. Chem. Lett.* 5 (1995) 2783–2788.
- [36] B.F. Mirjalili, L. Zamani, K. Zomorodian, S. Khabnadideh, Z. Haghhighijoo, Z. Malakotikhah, S.A. Ayatollahi Mousavi, S. Khojasteh, Synthesis, antifungal activity and docking study of 2-amino-4H-benzochromene-3-carbonitrile derivatives, *J. Mol. Struct.* 1116 (2016) 102–108.
- [37] A. Bolognese, G. Correale, M. Manfra, A. Lavecchia, O. Mazzoni, E. Novellino, P. La Colla, G. Sanna, R. Loddio, Antitumor agents. 3. Design, synthesis, and biological evaluation of new pyridoisoquinolindione and dihydrothienoquinolindione derivatives with potent cytotoxic activity, *J. Med. Chem.* 47 (2004) 849–858.
- [38] W.O. Foye, *Principi di Chemicco Farmaceutica*, Piccin, Padova, Italy, 1991 416.
- [39] L.L. Andreani, E. Lapi, On some new esters of coumarin-3-carboxylic acid with balsamic and bronchodilator action, *Bull. Chim. Farm.* 99 (1960) 583–586.
- [40] A.M. Shestopalov, Y.M. Litvinov, L.A. Rodinovskaya, O.R. Malyshev, M.N. Semenova, V.V. Semenov, Polyalkoxy substituted 4H-chromenes: synthesis by domino reaction and anticancer activity, *ACS Comb. Sci.* 14 (2012) 484–490.
- [41] Z. Cai, L.-J. Yan, A. Ratka, Telomere shortening and Alzheimer's disease, *NeuroMolecular Med.* 15 (2013) 25–48.
- [42] G. Shanthi, P.T. Perumal, An eco-friendly synthesis of 2-aminochromenes and indolyl chromenes catalyzed by  $\text{InCl}_3$  in aqueous media, *Tetrahedron Lett.* 48 (2007) 6785–6789.
- [43] Y.-M. Ren, C. Cai, Convenient and efficient method for synthesis of substituted 2-amino-2-chromenes using catalytic amount of iodine and  $\text{K}_2\text{CO}_3$  in aqueous medium, *Catal. Commun.* 9 (2008) 1017–1020.
- [44] A. Solhy, A. Elmakssoudi, R. Tahir, M. Karkouri, M. Larzek, M. Bousmina, M. Zahouily, Clean chemical synthesis of 2-amino-chromenes in water catalyzed by nanostructured diphosphate  $\text{Na}_2\text{CaP}_2\text{O}_7$ , *Green Chem.* 12 (2010) 2261–2267.
- [45] Y. Essamlali, O. Amadine, H. Maati, K. Abdelouahdi, A. Fihri, M. Zahouily, R.S. Varma, A. Solhy, Highly efficient one-pot three-component synthesis of naphthopyran derivatives in water catalyzed by phosphates, *ACS Sustain. Chem. Eng.* 1 (2013) 1154–1159.
- [46] N. Golari, M. Rahimizadeh, M. Bakavoli, E. Rezaei-Seresht, KG-60-piperazine as an efficient heterogeneous catalyst for three-component synthesis of 2-amino-2H-chromenes, *Res. Chem. Intermed.* 41 (2015) 6023–6032.
- [47] M. Zendejdel, M.A. Bodaghifard, H. Behyar, Z. Mortezaei, Alkylaminopyridine-grafted on HY zeolite: preparation, characterization and application in synthesis of 4H-Chromenes, *Microporous Mesoporous Mater.* 266 (2018) 83–89.
- [48] M.M. Heravi, K. Bakhtiari, V. Zadsirjan, F.F. Bamoharram, O.M. Heravi, Aqua mediated synthesis of substituted 2-amino-4H-chromenes catalyzed by green and reusable Preyssler heteropolyacid, *Bioorg. Med. Chem. Lett.* 17 (2007) 4262–4265.
- [49] J. Mondal, A. Modak, M. Nandi, H. Uyama, A. Bhaumik, Triazine functionalized ordered mesoporous organosilica as a novel organocatalyst for the facile one-pot synthesis of 2-amino-4H-chromenes under solvent-free conditions, *RSC Adv.* 2 (2012) 11306–11317.
- [50] M. Mogharabi-Manzari, M.H. Ghahremani, T. Sedaghat, F. Shayan, M.A. Faramarzi, A Laccase heterogeneous magnetic fibrous silica-based biocatalyst for green and one-pot cascade synthesis of chromene derivatives, *Eur. J. Org. Chem.* 2019 (2019) 1741–1747.
- [51] S.K. Kundu, J. Mondal, A. Bhaumik, Tungstic acid functionalized mesoporous SBA-15: a novel heterogeneous catalyst for facile one-pot synthesis of 2-amino-4H-chromenes in aqueous medium, *Dalton Trans.* 42 (2013) 10515–10524.
- [52] Z. Arzhegar, V. Azizkhani, S. Sajjadifar, M.H. Fekri, Synthesis of 2-amino-4H-chromene derivatives under solvent-free condition using MOF-5, *Chem. Methodol.* 3 (2019) 251–260.
- [53] M. Fallah, S. Sohrabnezhad, M. Abedini, Synthesis of chromene derivatives in the presence of mordenite zeolite/MIL-101 (Cr) metal-organic framework composite as catalyst, *Appl. Organomet. Chem.* 33 (2019), e4801.
- [54] T. Hajjashrafi, M. Karimi, A. Heydari, A.A. Tehrani, Erbium-organic framework as heterogeneous Lewis acid catalysis for Hantzsch coupling and tetrahydro-4H-chromene synthesis, *Catal. Lett.* 147 (2017) 453–462.
- [55] S.K. Kundu, A. Bhaumik, A triazine-based porous organic polymer: a novel heterogeneous basic organocatalyst for facile one-pot synthesis of 2-amino-4H-chromenes, *RSC Adv.* 5 (2015) 32730–32739.
- [56] C. Wang, X. Liu, N. Keser Demir, J.P. Chen, K. Li, Applications of water stable metal-organic frameworks, *Chem. Soc. Rev.* 45 (2016) 5107–5134.
- [57] A.P. Abbott, G. Capper, D.L. Davies, R.K. Rasheed, V. Tambyrajah, Novel solvent properties of choline chloride/urea mixtures, *Chem. Commun.* (2003) 70–71.
- [58] D. Azarifar, R. Ghorbani-Vaghei, S. Daliran, A.R. Oveisi, A multifunctional zirconium-based metal-organic framework for the one-pot tandem photooxidative Passerini three-component reaction of alcohols, *ChemCatChem* 9 (2017) 1992–2000.
- [59] M.J. Katz, J.E. Mondloch, R.K. Totten, J.K. Park, S.T. Nguyen, O.K. Farha, J.T. Hupp, Simple and compelling biomimetic metal-organic framework catalyst for the degradation of nerve agent simulants, *Angew. Chem. Int. Ed.* 53 (2014) 497–501.
- [60] M. Pintado-Sierra, A.M. Rasero-Almansa, A. Corma, M. Iglesias, F. Sánchez, Bifunctional iridium-(2-aminoterephthalate)-Zr-MOF chemoselective catalyst for the synthesis of secondary amines by one-pot three-step cascade reaction, *J. Catal.* 299 (2013) 137–145.
- [61] S. Daliran, M. Ghazagh-Miri, A.R. Oveisi, M. Khajeh, S. Navalón, M. Álvaro, M. Ghaffari-Moghaddam, H. Samareh Delarami, H. García, A pyridyltriazol functionalized zirconium metal-organic framework for selective and highly efficient adsorption of palladium, *ACS Appl. Mater. Interfaces* 12 (2020) 25221–25232.
- [62] M. Sarker, J.Y. Song, S.H. Jhung, Carboxylic-acid-functionalized UiO-66-NH<sub>2</sub>: a promising adsorbent for both aqueous- and non-aqueous-phase adsorptions, *Chem. Eng. J.* 331 (2018) 124–131.
- [63] A.A. Tehrani, S. Abedi, A. Morsali, J. Wang, P.C. Junk, Urea-containing metal-organic frameworks as heterogeneous organocatalysts, *J. Mater. Chem. A* 3 (2015) 20408–20415.
- [64] C. Du, B. Zhao, X.-B. Chen, N. Birbilis, H. Yang, Effect of water presence on choline chloride-2urea ionic liquid and coating platings from the hydrated ionic liquid, *Sci. Rep.* 6 (2016) 29225.
- [65] Z. Zhang, H. Yuan, An alumina-coated UiO-66 nanocrystalline solid superacid with high acid density as a catalyst for ethyl levulinate synthesis, *J. Chem. Technol. Biotechnol.* n/a.
- [66] A. Zhu, T. Jiang, B. Han, J. Zhang, Y. Xie, X. Ma, Supported choline chloride/urea as a heterogeneous catalyst for chemical fixation of carbon dioxide to cyclic carbonates, *Green Chem.* 9 (2007) 169–172.
- [67] S. Khandelwal, Y.K. Tailor, M. Kumar, Deep eutectic solvents (DESs) as eco-friendly and sustainable solvent/catalyst systems in organic transformations, *J. Mol. Liq.* 215 (2016) 345–386.
- [68] L.S. Longo Jr., M.V. Craveiro, Deep eutectic solvents as unconventional media for multicomponent reactions, *J. Braz. Chem. Soc.* 29 (2018) 1999–2025.